

Manufacturing Technology

**Kenneth L. Blaedel,
Thrust Area Leader**

This is an informal report intended primarily for internal or limited external distribution. The opinions and conclusions stated are those of the author and may or may not be those of the Laboratory.

Work performed under the auspices of the U.S. Department of Energy by Lawrence Livermore National Laboratory under Contract W-7405-Eng-48.

February 1997

Disclaimer

This document was prepared as an account of work sponsored by an agency of the United States Government. Neither the United States Government nor the University of California nor any of their employees, makes any warranty, express or implied, or assumes any legal liability or responsibility for the accuracy, completeness, or usefulness of any information, apparatus, product, or process disclosed, or represents that its use would not infringe privately owned rights. Reference herein to any specific commercial products, process, or service by trade name, trademark, manufacturer, or otherwise does not necessarily constitute or imply its endorsement, recommendation, or favoring by the United States Government or the University of California. The views and opinions of authors expressed herein do not necessarily state or reflect those of the United States Government or the University of California, and shall not be used for advertising or product endorsement purposes.

This report has been reproduced
directly from the best available copy.

Available to DOE and DOE contractors from the
Office of Scientific and Technical Information
P.O. Box 62, Oak Ridge, TN 37831
Prices available from (615) 576-8401, FTS 626-8401

Available to the public from the
National Technical Information Service
U.S. Department of Commerce
5285 Port Royal Rd.,
Springfield, VA 22161

THRUST AREA REPORT • UCRL-ID-125473

Manufacturing Technology

**Kenneth L. Blaedel,
Thrust Area Leader**

Reprinted from Engineering Research, Development and Technology
FY 96 UCRL 53868-96

February 1997



Kenneth L. Blaedel, Thrust Area Leader

The mission of the Manufacturing Technology thrust area at Lawrence Livermore National Laboratory (LLNL) is to have an adequate base of manufacturing technology, not necessarily resident, to conduct future business.

Our specific goals continue to be (1) to develop an understanding of fundamental fabrication processes; (2) to construct general purpose process models that will have wide applicability; (3) to document our findings and models in journals; (4) to transfer technology to LLNL programs, industry, and colleagues; and (5) to develop continuing relationships with the industrial and academic communities to advance our collective understanding of fabrication processes.

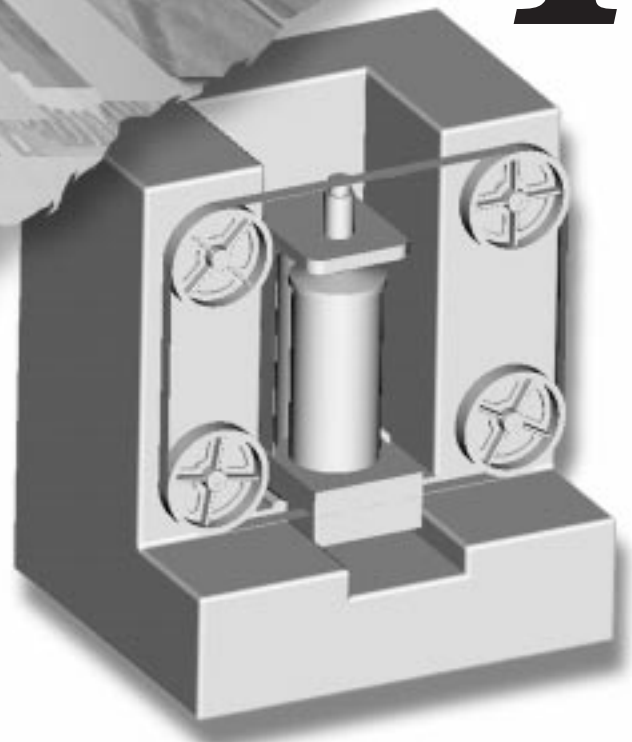
The environment in which the thrust area operates includes Laboratory Directed Research and Development (LDRD), Cooperative Research and Development Agreements (CRADAs) with outside industry, and development work that is performed

and paid for within an LLNL program. In general, LDRD incorporates the higher risk research associated with manufacturing technology, while the CRADAs embody the lower-risk reduction-to-practice associated with industry. The ideas developed in the thrust area fall somewhere in between.

Our niche continues to be bringing our strengths in precision engineering to bear on problems in manufacturing, particularly trying to increase the precision-to-cost ratio of some of the processes and devices that we think important to our future. The motivation for this is that the demand for the utmost in precision is now accompanied by a demand for less expensive precision. CRADAs have presented this demand over the past few years. Recently, as support for CRADAs has waned, work for LLNL programs has waxed, with surprisingly similar demands. Thus, application of manufacturing technology, the lower-risk end of the spectrum, has shifted from CRADA partners to LLNL programs.

Manufacturing Technology

4



4. Manufacturing Technology

Overview

Kenneth L. Blaedel, Thrust Area Leader

Design of a Precision Saw for Manufacturing

Jeffrey L. Klingmann.....4-1

Deposition of Boron Nitride Films via PVD

David M. Sanders, Steven Falabella, and Daniel M. Makowiecki.....4-5

Manufacturing and Coating by Kinetic Energy Metallization

T. S. Chow.....4-9

Magnet Design and Applications

Thomas M. Vercelli4-15

Design of a Precision Saw for Manufacturing

Jeffrey L. Klingmann
Manufacturing and Materials Engineering Division
Mechanical Engineering

A precision saw, similar in concept to a common bandsaw, for slicing crystallographic materials is investigated. The saw, which uses a hydrodynamic bearing for improved cut precision, would allow a significant reduction in the number of secondary finishing operations in the production of, for instance, KDP crystals for the Lawrence Livermore National Laboratory (LLNL) Laser Program, and silicon wafers for the semiconductor industry.

Introduction

The precision slicing of crystalline materials is a technology that presents an opportunity to reduce the cost of fabricating KDP crystals for the National Ignition Facility (NIF). If the precision of the first processing stage of the KDP boule can be improved significantly, costs will be reduced through elimination of subsequent fabrication steps for the approximately 800 required crystals.

A similar opportunity exists in the semiconductor industry, which is currently increasing the diameter of the typical silicon wafer from 200 to 300 mm, and planning a further increase to 400 mm. Drivers in this process are not only precision, but also reduced kerf width and high throughput. We have instituted a project to develop a precision saw to meet the needs of these two applications.

Progress

The three focus areas of the Precision Saw Project are blade development, prototype testing and conceptual machine design. During FY-96, progress was made in blade development and in the design features of a production machine. Testing of prototypes is discussed in the Future Work section below.

Blade Development

The hydrodynamic bandsaw blade design can be separated into the hydrodynamic lubrication analysis of the bearing and the cutting features on the leading edge of the blade. In hydrodynamic design, we have continued work started in FY-95 with the

modeling of the fixed-incline bearing, and extended this effort to include a parallel-step bearing design that will be much easier to fabricate.

Since existing designs use only tension to maintain blade straightness in the cut, the tensioned blade or wire provides a useful comparison for the hydrodynamic design.

Using 2-D hydrodynamic models,¹ we calculated the restorative force as a function of disturbance offset (**Fig. 1**) for the two bearings and the tensioned blade. The slopes of these curves represent the stiffness of the blade in the cut. The hydrodynamic bearing in this calculation has 12- μm -tall features and a nominal 50- μm gap, while the tension on the blade or wire is assumed to be 70,000 N.

Since the models used are only 2-D and do not include the effects of leakage to the sides of the wedge (to the front and back of the blade), the actual stiffness of the hydrodynamic bearing would

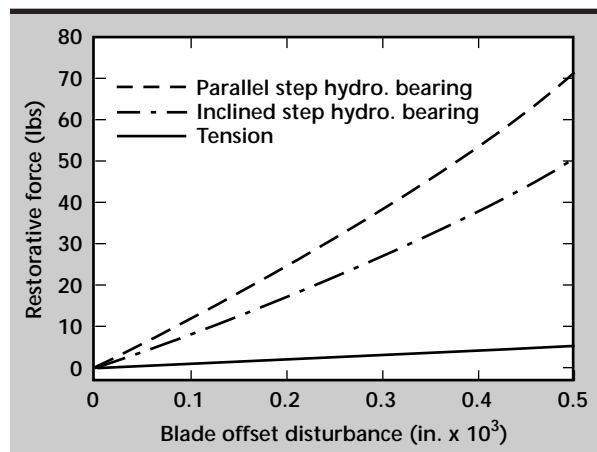


Figure 1. Comparison of restorative forces on the blade.

be somewhat less than indicated in **Fig. 1**. However, the high stiffness of the proposed blade design, compared to just a tensioned blade, should minimize the effect of disturbances that would cause poor cut precision. Beyond these two cases, computational fluid dynamics (CFD) methods will have to be used to examine 3-D effects and to consider alternative bearing designs such as the “herringbone.”

The other aspect of the bandsaw blade is the design of the cutting edge and how this feature is fabricated. While the cutting parameters such as diamond size, surface speed, and feed-rate are important, just as critical is a reliable method of fabricating the cutting edge on a metal band with the bearing features previously etched on its surfaces. It is desirable that the width of the cutting edge be small to keep the kerf small, and that the diamonds on the edge be durable for reasonable productivity and cost-effectiveness. Also, the diamond coating should be uniform and symmetric on the blade to minimize cutting errors.

Three methods of producing the blade cutting edge were investigated. The first is the industry standard which is to electroplate nickel with diamond onto the edge of the blade. The limitations to this process are that typically large diamonds are used in a fairly thick layer, resulting in a larger kerf. Additionally, the diamonds are held physically into the nickel coating and are therefore easily detached from the blade.

The second method uses a process developed at LLNL to apply a single layer of diamonds to a substrate with a much stronger chemical bond. This method has been tested for other applications and produces a very thin, durable abrasive coating due to the chemical bond to the substrate. Investigations into the applicability of this method are on-going.

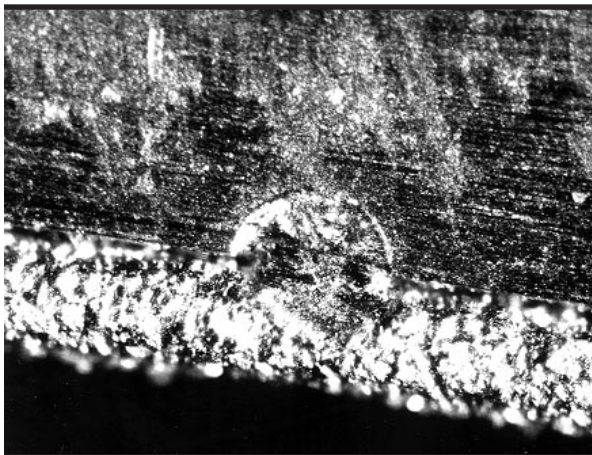


Figure 2. Diamond-impregnated wire brazed to a stainless steel substrate (100 \times).

Finally, the third method is to physically bond a fine diamond-impregnated wire to the leading edge of the blade. Typical wire saws for the silicon wafer saw industry use a loose abrasive process. However, for other applications, Laser Technology Inc. produces a fixed abrasive wire. **Figure 2** shows a 250- μm wire with 15- μm diamond abrasive that was laser-brazed to the leading edge of a 100- μm stainless steel band. Cutting and durability tests are continuing on this sample, but it seems to be a viable option for a prototype saw blade to test, for instance, the effect of diamond grit size on performance. The chemically-bonded process is preferred for production blades.

Conceptual Machine Design

Attempting the design of a production precision saw at this early stage of the project forces designers and engineers to consider the entire problem of slicing crystalline materials, not allowing a narrow focus on only a few aspects. Additionally, a conceptual machine design has use in describing various aspects of the project to industrial contacts. The following list of machine design requirements and features have been identified.

- 1) Boule and wafer fixturing. Due to the potential for large forces being generated by the hydrodynamic blade bearing, the wafer must be substantially supported to prevent fracture. If this fixturing for the boule and wafer can be a structurally stiff loop that also contains a guide for the blade entering and exiting the boule, the wafer thickness variation and flatness can be improved. This fixturing must also allow the boule to be oriented so that cuts are made in the proper relation to the crystallographic plane.
- 2) Axis configuration. Traditional bandsaws have the blade wheels rotating about horizontal axes and the part translating on a linear horizontal axis. Our current thinking maintains this approach but uses four wheels and slices on the blade span between the bottom two wheels; hence the symmetry axis of the boule is now vertical, and parts may be removed from the bottom of the saw.
- 3) Immersed cutting. To maintain a constant water supply to the hydrodynamic blade bearing, it is preferable to immerse the cutting region in a bath of cutting fluid. Of course, a consideration is the frictional loss due to the viscous fluid action on the rotating wheels.
- 4) Productivity. For a silicon slicing application, the saw must have high throughput to match competitive technologies. The productivity of

the current machine design will likely come from its improved performance, obviating the need for secondary finishing steps. The current industry solution for 300-mm silicon wafers is the diamond slurry wire saw which appears to be capable of producing 300 to 3000 wafers/day (12 to 120 wafers/h). It appears likely that a precision saw can be designed to cut multiple (5 to 10) boules simultaneously, so that a throughput of 60 wafers/h is possible.

- 5) Cutting force support. A current unknown is how much force is generated in the in-feed direction during cutting. This force must be resisted to keep the blade on the wheels. The desired solution is to use actively controlled magnets and a magnetic blade material to maintain blade position.

A simplified view of the proposed machine design incorporating these ideas is shown in **Fig. 3**.

Future Work

The most critical task to pursue in the future is to test the hydrodynamic and cutting characteristics of the blade. The current plan begins with blade testing in a guide with the hydrodynamic features in replaceable guides and mechanical wheel bearings. The next steps would be to incorporate the desired features into the blade with a photo-etching process and to design and fabricate hydrostatic bearings for the blade wheels. Finally, a cutting blade would be tested on a machine with a linear axis to translate the boule.

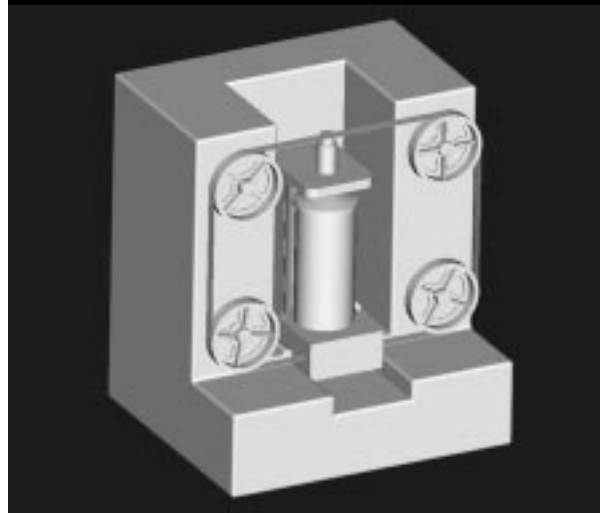



Figure 3. Simplified view of a conceptual production precision saw.

Modeling of the hydrodynamic features should continue with a CFD code to perform detailed design on both simple bearing configurations, such as the parallel and inclined step, and more advanced concepts such as a herringbone design. A conceptual machine design should also be developed to examine critical aspects of a production machine so that necessary concepts can be tested on a prototype machine.

References

1. Hamrock, B. J. (1994), *Fluid Film Lubrication*, McGraw Hill Co., New York, N.Y. 

Deposition of Boron Nitride Films via PVD

David M. Sanders and Steven Falabella
Material Fabrication Division
Mechanical Engineering

Daniel M. Makowiecki
Materials Science and Technology Division
Chemistry and Materials Science

A neutral beam-assisted deposition system that has demonstrated the potential of producing high-quality films at reduced stress was assembled and evaluated in a chamber in the Vacuum Processes Laboratory of Lawrence Livermore Laboratory (LLNL). Transparent boron nitride (BN) coatings were produced, with some varying crystal structure, as evidenced by absorption differences in FTIR scans of films produced with varying amounts of neutral bombardment. However, no conclusive evidence of the cubic phase was noted. The films produced were very adherent to silicon substrates and exhibited low residual stress, indicating that this process may be able, with additional optimization, to produce technologically useful cubic BN films.

Introduction

One of the strengths of LLNL in the precision manufacturing field is its diamond turning capability. Rotationally symmetric workpieces can be machined to tolerances of just a few microinches. However, one of the severe limitations of this technology is that only a select few non-ferrous metals (including copper, gold, aluminum, and nickel) can be machined with surface roughness less than 5 nm with a single-crystal diamond tool. The high quality workpiece surface results from the very sharp initial edge of the single-crystal diamond, and the resistance of the diamond edge to wear against these metals. In contrast, carbide-forming metals such as steel, titanium, and beryllium cannot be similarly machined, because they cause excessive chemically-induced wear of the diamond.

There is great demand for precision turning of workpieces made from carbide-forming metals. Within LLNL, for example, precision components of steel and beryllium are of great interest. Within the commercial sector, the steel bearing process would benefit economically if bearings could be turned instead of ground. Within the Department of Defense, there are many current and future components which would benefit from high precision turning, such as mirrors machined directly from silicon.

Boron-based coatings are also of interest for other applications, including electronics, optical filters, wear-resistance, and high-hardness applications.

Our goal for this project is to turn high-precision, very smooth surfaces on carbide-forming materials, particularly steel, through the use of a hard-coated tool. This goal is distinguished from many other hard-coated tool efforts that are directed not at the finishing stage, but rather at the intermediate or roughing stage of manufacture. In this finishing domain, a coating thickness of perhaps 1 μm is considered a thick coating, and a tool edge radius of 1 μm is considered dull. The reward for success is that the large investment we already have in the infrastructure to perform diamond turning could be brought to bear on other desirable materials with a small incremental cost of a coated tool.

The most successful method, ion-beam assisted deposition, has a problem with stress delamination limiting the thickness of films. We used two methods to produce BN films. The first, sputtering of a boron target in a nitrogen atmosphere is a continuation of last year's work, and the second, e-beam evaporation of boron while simultaneously bombarding the substrate with an energetic, neutral nitrogen beam, is documented in this report. We will refer to the latter approach as neutral-beam assisted deposition (NBAD). The sputtering work was done in

LLNL's Chemistry and Materials Science Department, while the NBAD work was done in its Vacuum Processes Laboratory.

Progress

A NBAD system that has demonstrated the potential of producing high-quality films at reduced stress¹ was assembled and evaluated in a chamber in the Vacuum Processes Laboratory at LLNL. An



Figure 1: Photograph of apparatus used for NBAD of BN films.

Ion Tech 3-cm-diameter ion source and custom neutralizer cone was used to focus the neutral nitrogen onto the substrates held on a radiatively-heated stage. A Balzers e-beam system was installed in the chamber to evaporate the boron. These two systems were assembled for the first time in this chamber. Since it took much effort to get to a point of reliable operation there was insufficient time to optimize the deposition process.

Transparent BN coatings were produced, with some varying crystal structure as evidenced by absorption differences in FTIR scans of films produced with varying amounts of neutral bombardment. However, no conclusive evidence of the cubic phase was noted. The films produced were very adherent to silicon substrates and exhibited low residual stress, indicating that this process may be able, with additional optimization, to produce technologically useful cubic BN films.

Description of Process

The formation of cubic BN (c:BN) has been shown to require three conditions: a source of boron, a source of energetic nitrogen, and a substrate temperature in the range of 400 to 800 °C. A photograph of the system is shown in **Fig. 1**. A Balzers e-beam evaporator was used as the source of boron. The evaporation rate was monitored and controlled by an Inficon IC6000 controller and quartz crystal monitor placed near the substrate. The evaporation rate was varied in the 0.5 to 2.0 Å/s range for this series of experiments.

The energetic nitrogen was supplied as a neutral beam. This beam was produced by directing an ion beam onto the inside of a cone. An Ion Tech 3-cm, gridded ion source was used, with hollow cathode

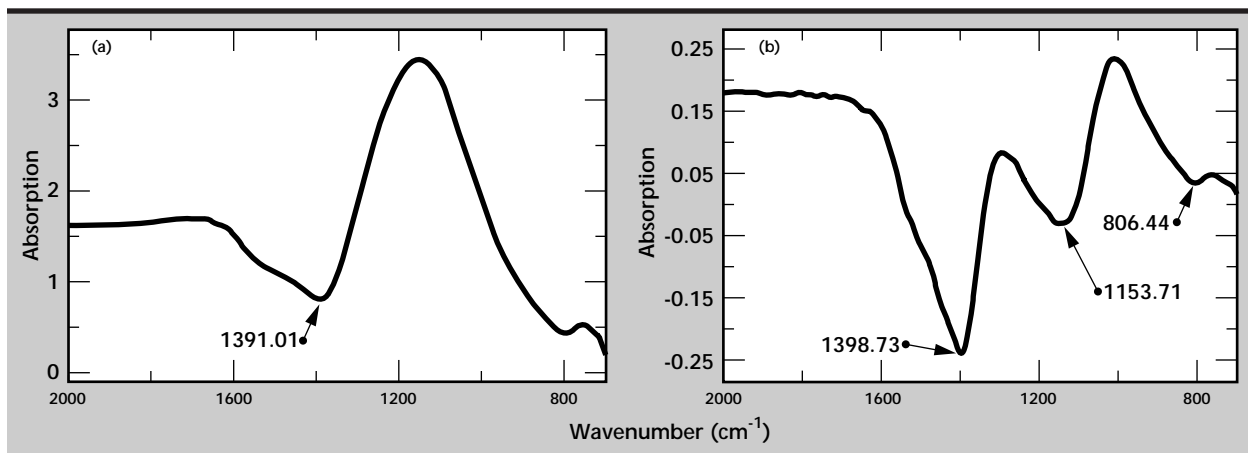


Figure 2. (a) FTIR scan of typical BN film produced by NBAD system. The absorption near 1390 cm⁻¹ is indicative of the hexagonal phase. (b) FTIR scan of an area that shows absorption near 1150 cm⁻¹, which is evidence of sp³ bonding.

plasma source using a 50/50 nitrogen/argon gas mix. Inside the outer cone, there was a smaller, inverted cone to block all line of sight to the substrate. The cone provides surface neutralization of the ion beam, while the particle energy is reduced only slightly due to the glancing angles the ion beam makes with the cones. The ion energy was varied from 300 to 550 eV and ion currents from 25 to 50 mA over the course of these experiments.

The 2-in. silicon wafers used as substrates were held at the exit of the neutralizer cone, in the evaporation plume of the boron source, on a heated stage. The temperature of the stage was varied from 400 to 550 °C for this series of experiments. The stage has the capability of biasing with either rf or dc, but this was not used for this work, as the goal was to use neutral nitrogen bombardment of the substrate.

Results

As noted above, transparent BN films were produced using the above equipment over a fairly wide range of conditions, but in the limited time available, conditions that produce the cubic phase were not found. The crystal structure of the films was determined using the absorption characteristics measured using FTIR spectrometry in the 700 to 2000 cm^{-1} range. A representative scan is shown in **Fig. 2a**. Most of the films demonstrated a large, broad absorption at 1390 cm^{-1} and smaller peak near 800 cm^{-1} , indicative of sp^2 (hexagonal) bonded BN. As shown in **Fig. 2b**, one sample exhibited

absorption at 1150 cm^{-1} , which is close to the cubic phase signature of 1060 cm^{-1} , but we feel that the shift is too great to be explained by intrinsic stress, and may be due to a wurtzite phase.² Although it is sp^3 bonded, this phase is metastable and not the hard, cubic phase useful in tool bit coatings.


Conclusions

Although not demonstrated using NBAD, there were indications that the system could produce c:BN films of good adherence and low enough stress to make coatings thick enough for tool bit use.

Acknowledgments

We wish to thank R. Sanborn of Analytical Sciences Division for producing the FTIR scans of our films, and S. Bryan of MMED for assembling and troubleshooting the Balzers e-beam system.

References

1. Lu, M, A. Bousetta, R. Sukach, A. Bensaoula, K. Walters, K. Eipersmith, and A. Schultz (1994), "Growth Of Cubic Boron Nitride On Si(100) By Neutralized Nitrogen Ion Bombardment," *Applied Physics Letters*, Vol. **64**, (12), pp. 1514–1516.
2. Mirkarimi, P. B., K. F. McCarty, and D. L. Medlin, "Critical Review of Advances in Cubic Boron Nitride," to be published in *Science & Technology of Hard Coatings*, Sundgren and Barnett, Editors. 

M

anufacturing and Coating by Kinetic Energy Metallization

T. S. Chow
*Defense Technologies Engineering Division
 Mechanical Engineering*

We have performed systematic laboratory experiments and modeling analyses to demonstrate that (1) it is feasible to form thin and thick deposits by kinetic energy metallization (KEM) using various metal powders onto several types of substrates; (2) very low as-deposited porosity can be achieved by using fine ($<10\ \mu\text{m}$) to ultra fine ($<3\ \mu\text{m}$) powders; (3) KEM deposition rates are favorable for thick buildup for practical applications; and (4) the thick deposits will require post-KEM processes for improvement in both density and tensile properties. In addition, computer modeling predicts that the magnitude of the impact velocity is an important factor and that high deformations are produced in both impacting particles and target materials after impact. Features in the micrographs are consistent with these predictions.

Introduction

KEM is a low-bulk temperature coating process not requiring the introduction of thermal energy. Bonding energy is induced by high-speed impact of fine metal particles on a substrate. KEM is different from the conventional thermal spray coating processes in which the metal particles are heated to the liquid state and sprayed by a moderate- to high-speed carrier gas at the substrate to produce coatings. The processes are high-temperature operations. KEM is therefore very attractive for near net shape products.

ITI (Las Cruces, NM) was the first company in the U. S. to produce thin coating deposition samples through KEM technology and has applied for the patent rights. A group of Russian researchers have published similar work¹ called "cold gas-dynamic deposition."

Our objectives are to demonstrate the technical feasibility of the KEM process through a parametric experimental study in a controlled environment and to establish better understanding of the particle-to-substrate interaction mechanisms. The coating and forming experiments based on a mutually agreed upon test matrix were performed by ITI under a contract with Lawrence Livermore National Laboratory (LLNL).

ITI produced a set of thin coatings, on the order of 10's of mils, from which process parameters were selected to generate three bulk (thick) samples, Ti, Cu, and Zn, for further testing and analyses at LLNL.

Preliminary finite element analyses of the impact process were carried out at LLNL. The goal of the analytical studies is to determine the effects of particle velocity, size, material, and substrate material.

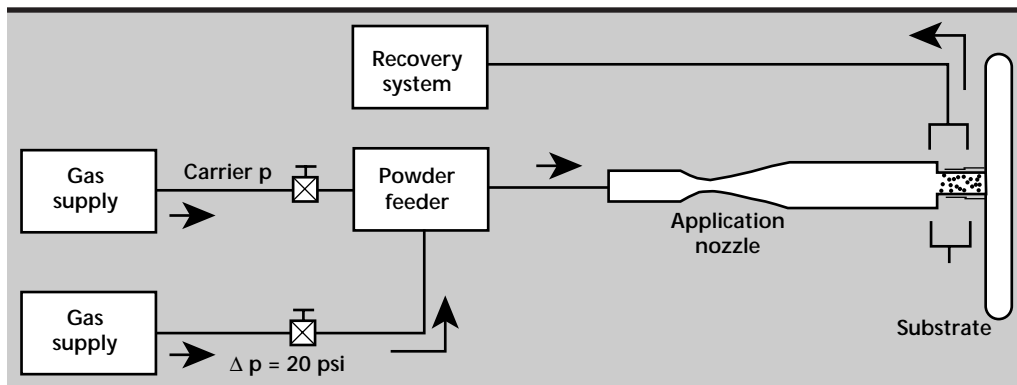


Figure 1. Schematic representation of the KEM system.

Progress

KEM Test System and Process Description

A schematic of the KEM system is shown in Fig. 1. The system consists of a supersonic nozzle

for driving μm -sized particles to speeds in excess of 300 m/s and a recovery hood for the over-sprayed powder. The gas source used two K-bottles of commercial grade He, regulated to nozzle inlet pressures of 500 psig or less. The fluidizing gas pressure driving the feeder was regulated to a Δp of 20

Table 1. KEM test matrix based on six parameters.

Parameters	Lower bound	Upper bound	Increment	Bulk samples
1 Substrate hardness	Al	Cu or Inconel-600		Al
2 Powder type: reactivity melting point hardness		Al Cu Ni Ti Zn		Cu Ti Zn
3 Powder size	<3 μm	<45 μm	3 sizes	<10 μm , 45 (Ti)
4 Gas type	N	He	2 gases	He
5 Nozzle inlet pressure	200 psig	450 psig	3 settings	200 to 300
6 Deposition duration	5 s	60 s	3 values	up to 60 s

Table 2. Summary of all runs using Al substrate.

Powder	Avg. deposition rate ($\mu\text{m}/\text{cm}^2\text{-s}$)	He gas (psig)	Porosity	Hardness RH, 15T	Base metal RH
Al (<10 μm)	13 \pm 7	200	<5%	71 \pm 2	77 \pm 2
Al (<10 μm)	6 \pm 5	450	<5%	72 \pm 2	
Al (20 μm), sph	99 \pm 20	200	5 to 10%	61 \pm 4	
Al (20 μm), sph	384 \pm 20	450	5 to 10%	64 \pm 3	
Cu (<10 μm)	8 \pm 3	100	<5%	77 \pm 3	76 \pm 1
Cu (<10 μm)	84 \pm 17	200	5.6 \pm 4.5	85 \pm 2	
Cu (<10 μm)	122 \pm 23	450	<5%	89 \pm 2	
Cu (<45 μm)	20 \pm 1	200	> 10%	76 \pm 2	
Cu (<45 μm)	59 \pm 6	450	> 10%	78 \pm 3	
Ni (<3 μm)	14 \pm 5	200	-	88 \pm 2	87 \pm 1 (Inconel-600)
Ni (<3 μm)	23 \pm 12	450	-	87 \pm 2	
Ni (<10 μm)	13 \pm 4	200	5 to 10%	88 \pm 4	
Ni (<10 μm)	44 \pm 7	450	-	92 \pm 1	
Ti (<45 μm)	29 \pm 7	200	18 \pm 4.5	78 \pm 3	80 \pm 1
Ti (<45 μm)	42 \pm 13	450	> 10%	83 \pm 6	
Zn (<10 μm)	82 \pm 8 to 160 \pm 44	200 to 450	<5%	63 \pm 4	
Zn (10 to 25 μm)	15 \pm 6 to 20 \pm 3	200 to 450	<5%	58 \pm 4	

to 30 psig above the process line. Nitrogen gas was periodically tested throughout the parametric study to determine if the KEM depositions were feasible with a lower expansion velocity gas.

The test matrix consists of the following parameters with a wide range of values: powder materials, powder sizes (commercial grades), carrier gases, pressures, and substrate materials based on hardness and deposition thickness (thin film and bulk samples, as summarized in **Table 1**).

Results

The detailed experimental data and results are given in ITI's final report.²

Table 2 summarizes the results for deposit on aluminum substrates, showing the effects of powder size, shape and gas pressure on the deposition rate, porosity, and hardness. The large uncertainties associated with the deposition rates were attributed to powder flow rate variations that were highly dependent on the powder properties and the feeder behavior. Generally, higher inlet pressures and smaller particles tended to increase the deposition rates. A few selected KEM depositions of various powders were made on substrates of Cu, Al, and Ni.

The micrographic characterization of all the samples listed in **Table 2** is included in Reference 1.

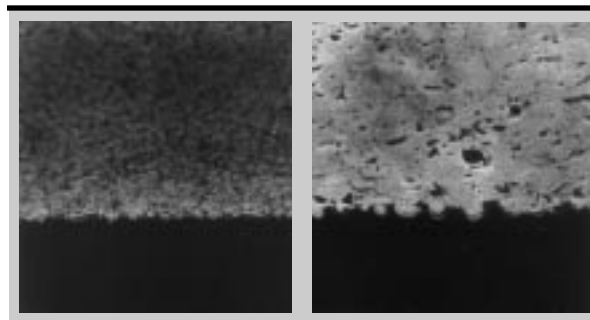


Figure 2. Micrographs of Cu on Al, <10 μm (a) and <45 μm (b).

Micrographic comparison of the particle size effects are shown in **Fig. 2**, for Cu (<10 μm) and Cu (<45 μm) on Al. The bulk and interfacial porosities were quite low (<5%) for the <10- μm Cu, while the <45- μm Cu exhibited moderate porosity (10 to 15%). The micrograph of a Cu-on-Cu (**Fig. 3**) showed a much lower level of interfacial porosity, as compared to a Cu-on-Al deposit under otherwise identical conditions, suggesting that similar metals form stronger bonding than dissimilar ones.

ITI generated the bulk (thick) samples (Cu, Ti, and Zn) on (1mm) Al (**Table 3**) using the parameters derived from the test matrix. All KEM bulk samples were fairly rough on the deposition side because of manually operated nozzle translation. The Cu and Ti bulk samples exhibited significant residual stress that resulted in bending of the samples. The Zn sample showed much less residual stress.

The post-KEM processes included annealing of the Cu sample, and annealing followed by HIP-ing of the Ti sample. These treatments greatly improved the mechanical properties of the deposits. **Table 4** is a summary of the analysis and testing results.

Annealing of KEM-deposited Cu had moderate reduction in porosity, (from 6% to 4%), and a slight decrease in hardness. Annealing and HIP-ing of the KEM-deposited Ti reduced the porosity from 17% to 0, and greatly increased the hardness.

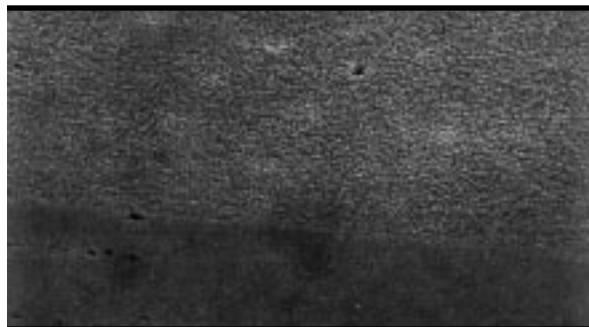


Figure 3. Micrograph of Cu on Cu.

Table 3. Bulk sample deposition parameters.

Bulk sample	Cu	Ti	Zn
Dimension	8.0 cm \times 1.6 cm \times 0.6 cm	8.0 cm \times 1.7 cm \times 0.5 cm	8.0 cm \times 1.8 cm \times 0.3 cm
Powder size	<10 μm	<45 μm	<10 μm
He pressure	300 psig	250 psig	300 psig
Height of curvature	3.0 mm	2.5 mm	0.5 mm
Radius of curvature	34	32	203

A tensile specimen (**Fig. 4**) machined from an annealed Cu sample was tested, with the result plotted in **Fig. 5**. It can be seen that, with 38 ksi ultimate stress at 0.75% elongation, the specimen was brittle but relatively strong.

Elemental analysis of the Cu sample shows that the bulk oxygen content was in line with the level of commercial grade Cu powders. The KEM process failed to purge out the oxide coating naturally occurring on the Cu particle surfaces.

Theoretical Modeling Analysis

There are three major aspects to the KEM phenomenon: (1) the gas dynamics of the supersonic, gas/solid jet impinging on the target that may or may not modify the shock waves in front of the

target; (2) the particle impact interaction processes at the surface; and (3) multiple impacts on (thick) KEM samples.

We have concentrated our analytical efforts^{3,4,5} on the last two problems, that is, the interaction of the particle with the solid target upon impact at high velocities, particularly the time dependent deformation characteristics of both the particles and the surface on impact. The axi-symmetric 2-D CALE code that can calculate deformation and moving stress waves in the materials at high strain rates was used.

We have made calculations for various particle-impact scenarios. Here we discuss several sample cases: Cu particle impact on an Al target at various velocities (200 m/s, 500 m/s, and 1,000 m/s); Cu particle impact on a Cu target at 1 km/s; and two Cu

Table 4. Bulk samples test summary.

	Treatment ⁽¹⁾	Rockwell hardness ⁽²⁾	Density	Tensile property	Machine-ability	Oxygen content
Cu	As-deposited	87 (15T)	94%	—	poor	0.209% ± 0.057— comparable to general MSDS spec. for Cu powders
	Annealed	80 (15T)	96%	38 ksi 0.7% (ultimate)	good	
Ti	As-deposited	82 (15T)	82%	—	poor	—
	Annealed	32 (C)	93%	—	poor-fair	
	HIP'ed	38 (C)	100%	—	fair	
Zn	As-deposited	74 (15T)	96%	—	fair	—

(1) Annealing condition: 2/3 melting temperature for 3 h; HIP condition: 15 ksi at 1000 °C for 3 h.

(2) [15T] is the Rockwell superficial hardness: max. scale = 92.5, equivalent to 19.9 on [C] scale.

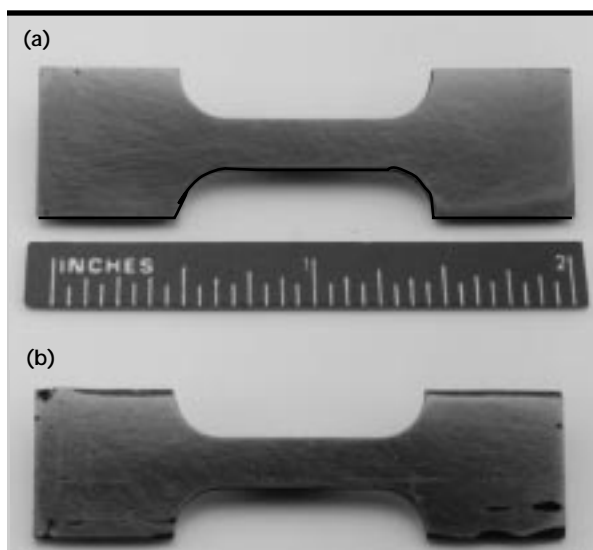


Figure 4. Annealed KEM-deposited Cu tensile specimen.

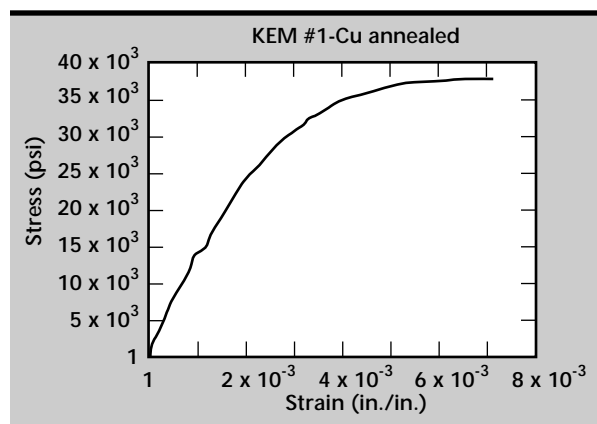


Figure 5. Stress/Strain of annealed KEM-deposited Cu.

particles impinging on an Al target at 1 km/s. The model assumes a moving particle (a cylindrical disk), about to strike a target at $t = 0$. Due to axisymmetry, only the top half of the field is needed in the simulation.

Case A: Effects of Particle Impact Velocity on Particle/Target Interaction. The deformation patterns of the Cu and Al materials at $t = 0.36 \mu\text{s}$ after impact, when the impact velocity was 200 m/s, resulted in only a small amount of deformation. When the impact velocity was increased to 500 m/s, greater deformation took place. The stress waves in the Al travel first as compressive and then relieving tensile, so that the dilation of the material brings about the bulging crater-like protrusions around the impacting Cu particle.

When the impact velocity is raised to 1,000 m/s, which is a realistic velocity considering the high Mach number and velocity for the He carrier gas, our results show marked penetration of the particle as well as fragmentation of the materials. These analytical predictions show indentations and detachment of the target materials that resemble those found in the ITI test samples.

Case B: Cu Particle Impact on Cu Target. We consider this case to determine if there are any differences in impact response of like materials. The results at $t = 0.24 \mu\text{s}$ after impact for the deformations in both the particle and the target show that these deformations are less than those for Cu on Al at $t = 0.24 \mu\text{s}$ after impact at 1,000 m/s, signifying that Al deforms more readily than Cu when struck by a Cu particle.

Case C: Two Cu Particles on a Cu Target. The initial configuration at $t = 0$ is that both particles are traveling toward the target at 1,000 m/s. At $t = 0.22 \mu\text{s}$ after impact, the first particle has already struck the target and has proceeded to interact with the target, while the second particle is still moving toward the target. The interaction shortly after the impact of the second particle shows that, at $t = 0.24 \mu\text{s}$, the penetration of the particles into the target at the centerline is now even greater and, in addition, the relieving tension waves cause the peripheral region of the target to protrude even more.

The velocity vectors show that the particles are still moving into the target, which will cause more deformation in both the target and the impacting particles at subsequent times.

Summary

This study has demonstrated that it is feasible to use the KEM process to deposit a wide range of metal powders to form both thin and thick coatings

on various substrates. The work also has validated KEM as an efficient method for spraying fine reactive and pyrophoric powders such as Ti, in an inert gaseous atmosphere without using high-vacuum deposition technology. Commercially available Ti powder was used.

Post KEM processes such as annealing and/or HIP-ing will greatly improve the mechanical properties of the KEM-produced free-standing components. For refurbishment or thin coating applications the post-processes may not be as important.

The effect of the measured residual oxide on the KEM material property is not well understood. But it does suggest that powder conditioning and/or *in-situ* generation of powder as an integral part of the KEM process should be studied.

We have done preliminary modeling analyses of the KEM phenomenon. The results indicate that impacts by solid particles at high velocities could cause deformations on both the incident particles and the target, and that the deformation in the latter material is qualitatively similar to that seen in the test samples.

Future Work

Our plans are to investigate the KEM process through experiments and modeling analyses to ultimately produce the optimum process conditions. The proposed tasks are:


- 1) conducting particle/target interaction experiments using a well-instrumented set-up, such as measuring the particle velocity and responses of both it and the target following the impact;
- 2) setting up a U-deposit facility and conducting U-6Nb experiments at LLNL to demonstrate the feasibility of the technology as applied to the U-alloy powder;
- 3) studying the effects of powder synthesis and conditioning on deposition; and
- 4) performing process modeling analyses.

Many important aspects of this complex metal-deposition phenomenon remain to be addressed, such as the interaction of the particles with each other and with the target in fully 3-D impact situations; the bonding process at the surface; and the behavior of the supersonic 2-phase (gas/solid) flow in front of the target and its effect on the shock wave and, especially, on the velocity distributions of the incident particles.

Acknowledgment

The author thanks S. W. Kang, who wrote the section on theoretical modeling analysis.

References

1. Alkhimov, A. P., V. F. Kosarev, and A. N. Papin (1990), "A Method of Cold Gas-Dynamic Deposition," *Soviet Physics Doklady*, **36**(12), pp. 1047–1049.
2. Tapphorn, R., and H. Gabel (1996), *Final Report—KEM Process Feasibility Study*, ITI, Las Cruces, New M.
3. Chow, T. S. (1996), "Manufacturing and Coating by Kinetic Energy Metallization (KEM)," *Progress Report for Manufacturing Thrust Area*, Lawrence Livermore National Laboratory, Livermore, Calif., March.
4. Chow T. S., and S. W. Kang (1996), *Preliminary Evaluation of KEM for Fabrication*, Lawrence Livermore National Laboratory, Livermore, Calif.
5. Tapphorn, R., and H. Gabel (1996), "Kinetic Energy Metallization Process Feasibility Study—Final Report," *Proceedings for the 12th General Meeting of JOWOG31, Livermore, Calif.*, ITI, Las Cruces, New M. 

Magnet Design and Applications

Thomas M. Vercelli
Applied Research Engineering Division
Mechanical Engineering

The primary goal of this project is to demonstrate and provide closure for the magnet design process used in the physics/accelerator community. The magnet design closure process compares the measured field to the design model for a magnet designed by the Accelerator Technology Engineering Group (ATEG) for the Stanford Linear Accelerator (SLAC). Revision of modeling techniques will be based on this data comparison to more accurately predict future magnet designs. A second goal is to produce a conceptual design of both a specific and generic magnetic field mapping device. A conceptual design for a specific magnet mapper is demonstrated by the application of an existing coordinate measuring machine at Lawrence Livermore National Laboratory (LLNL) to map a variety of standard dipole and quadrupole magnets. A conceptual design of a generic magnet mapper applicable to large scale magnets is demonstrated for the Muon Magnet of the PHENIX Detector project at the RHIC accelerator at Brookhaven National Laboratory (BNL).

Introduction

High-energy physics experiments frequently require large-aperture spectrometer magnets as well as high-quality bending and focusing magnets. Their magnetic fields vary widely in uniformity and symmetry and must be predicted very accurately. The sophisticated 2-D and 3-D computer simulations often must be verified by direct magnetic field measurements. Fully automatic positioning and magnetic field measuring equipment is required.

At present, there is no facility in the United States that has a full-fledged operating magnetic measurement laboratory. Without magnetic measuring capabilities, projects requiring magnets are relying on computer modeling techniques to accurately design the magnet to desired specifications. To date, no one has verified the accuracy of these models.

Our project looked at validation of the computational model used to design quadrupole focusing magnets for the B-Factory project at SLAC. The magnets were designed by the ATEG in ARED. Magnetic field measurement data was then compared to the predicted model by ATEG staff. Differences in the predicted fields versus the measured fields were assessed for computer code modeling accuracy.

This project also looked at a conceptual approach for mapping large-scale magnets by designing a scheme to map the PHENIX muon magnets. The approach can be applied to other large-scale magnets, such as the Compact Muon Solenoid (CMS) at CERN and the Main Injector Neutrino Oscillation Search (MINOS) at Fermi National Laboratory. A conceptual design for mapping bending and focusing magnets was done by adapting a coordinate measuring machine at LLNL to accurately position a probe arm and probe assembly inside a magnet bore.

Progress

Two modified PEP-I insertion quadrupole magnets will be used on the high-energy ring (HER) in the interaction region (IR) of the PEP-II asymmetric B-Factory at SLAC, with the name QF5 quadrupoles. The insertion quadrupoles were designed to provide an extremely uniform ($DB \leq 10^{-4}$) and pure ($B_1/B_2 \leq 10^{-4}$) quadrupole field.

Two-dimensional field calculations were performed using POISSON, a code widely used and accepted within the high-energy physics/accelerator community. Because the magnet geometry required a model with very small elements in a large cross-section, the code was challenged by the large size of the element count as well as by the necessity to have the

dimensions of air/iron interfaces on the order of the element dimensions. Magnetic measurements were performed at LLNL using a 161-mm diameter rotating “search” coil.

The measured multipole errors (normalized harmonics) were the same order of magnitude as the accuracy limitations of POISSON. Yet, a comparison between the calculated and measured major systematic multipoles ($n = 6,10$) indicates good agreement. The comparison indicates that POISSON is an excellent tool for magnet design and that the non-conventional use of single elements in air/iron interfaces was successful for this application.

A conceptual design of the PHENIX mapper was created, along with a parts list and cost estimate of fabrication, assembly, and testing. This design concept uses a combination of laser interferometry and CCD cameras as the tracking and positioning measurement system. Linear probe position (z-axis) is accomplished by a linear slide mounted on a boom. A cart carrying the Hall probes is attached to the linear slide. The boom rotates at one end and is attached to a wall crawler at the opposite end to achieve an x-y position (Fig. 1). The entire system is controlled by LABVIEW software.

This approach can be applied to other large-scale magnets such as the CMS. The probe-positioning system is specific to the PHENIX magnet volume, but the positioning concept, tracking, and control system can be generically applied to other magnets.

A conceptual design for using a coordinate measuring machine (CMM) as a mapping tool was created. This design uses the “DEA” CMM as the positioning device for the magnetic field measurement probes. A cantilevered probe arm assembly is attached to the CMM positioning head. The magnet to be mapped is placed on top of the granite table of the CMM. The CMM is programmed to position the field measuring probe inside the magnet bore. A data acquisition system (DAS) records the magnetic field.

The DAS is integrated with the CMM control system, so programmed movements of the measuring probe are coordinated with the field mapping. The CMM measures a reference target on the magnet to locate the center and axial location of the magnet bore. Probe position can then be programmed for very accurate probe placement during mapping (Fig. 2).

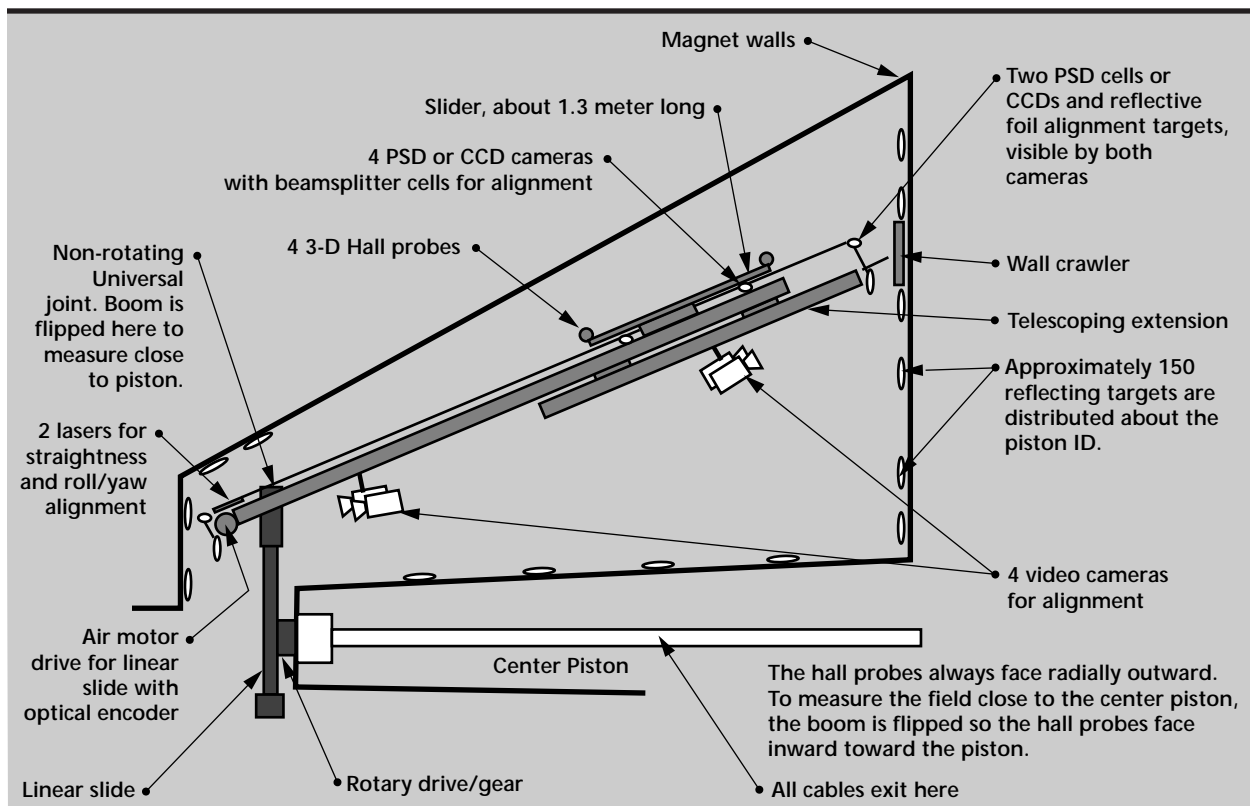


Figure 1. Conceptual design for PHENIX mapper.

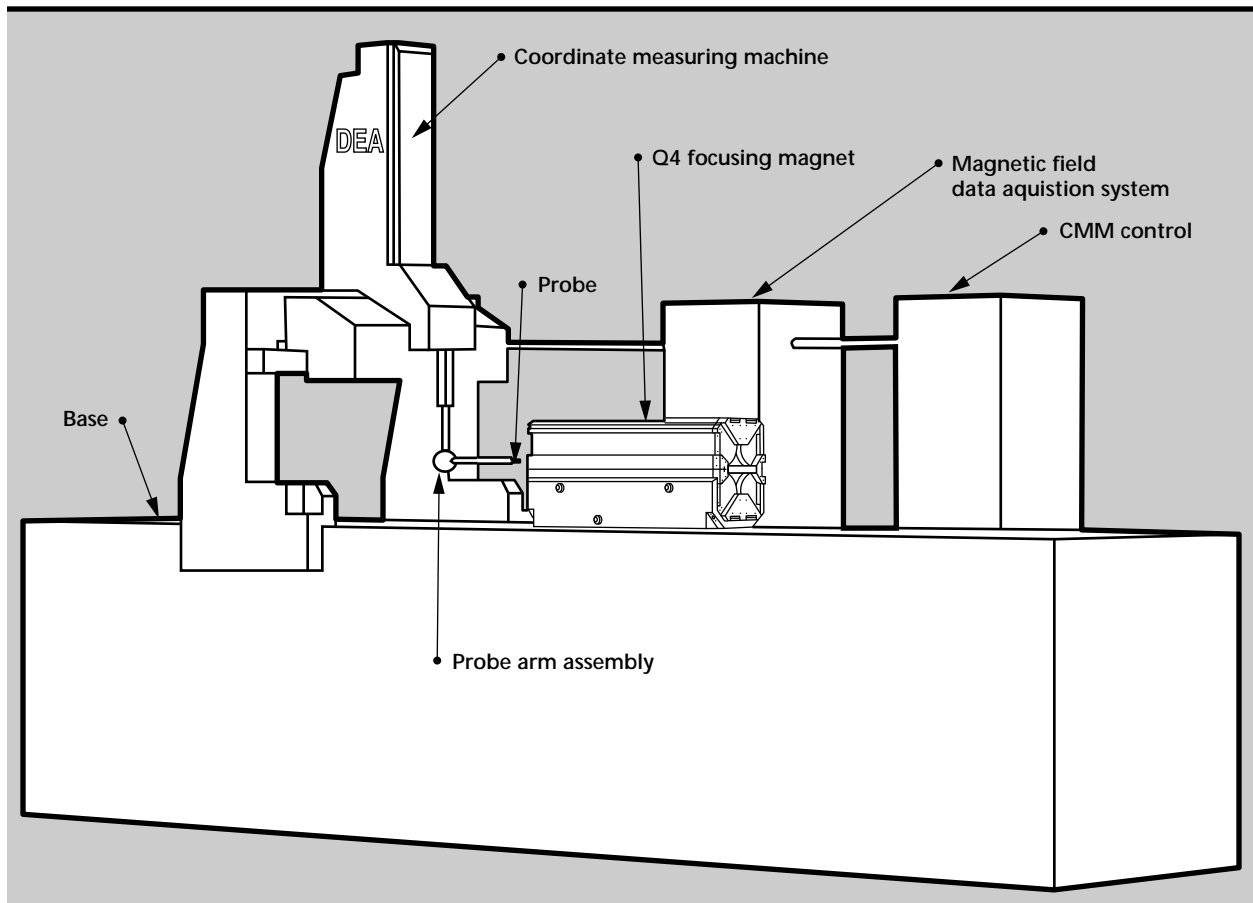


Figure 2. Conceptual design for coordinate measuring machine integrated with data acquisition system.

Future Work

Modeling validation has been done for only one magnet design. This is certainly not fully representative of the different magnet designs used. Further magnetic field data comparison should be done on a variety of magnets for increased confidence in the design code accuracy. Further code development is also necessary to calculate 3-D end effects of chamfers and shims, features currently modified empirically in the field.

Use of the CMM as a mapping tool will require a more detailed design and development effort in the areas of probe arm design; data acquisition and positioning integration; characterization of the probe arm assembly displacement errors due to magnetic field and thermal effects; and fabrication

and testing of the system. The completed product will then have a direct application to map magnets such as the HIF and AHF magnets.

Our specific mission can continue to evolve and broaden in scope. LLNL possesses core competencies and expertise that can be directly applied to the design, development, testing, manufacture, and implementation of magnetic field mapping systems. This thrust area can lead to the establishment of a magnetics engineering center at LLNL to support many programs as well as the high-energy physics/accelerator community.

Acknowledgment

The author thanks M. Kendall and J. Swan. 



Technical Information Department
Lawrence Livermore National Laboratory
University of California
Livermore, California 94551